International Journal of Thermophysics, Vol. 26, No. 4, July 2005 (© 2005)
DOI: 10.1007/s10765-005-6677-9

Three-Dimensional Finite-Element Analysis of High-Speed (Millisecond) Measurements[1]

E. Kaschnitz[2,3] and P. Supancic[4]

Millisecond pulse heating has become an established method to obtain accurate thermophysical property data for solid metallic materials at high temperatures. This technique is based on rapid resistive heating of a tubular- or rod-shaped specimen by an electrical current and simultaneously measuring the pertinent quantities with, at least, millisecond resolution. The temperature development during heating and subsequent cooling is usually measured by a high-speed pyrometer. For the case of a tubular specimen, the pyrometer is focused on a blackbody hole in the center part of the specimen. A three-dimensional finite-element analysis was used to investigate the limitations of the method used. A commercial program (ANSYS) was used for a highly nonlinear finite-element analysis taking into account temperature-dependent material properties as well as heat transport by radiation. Results of the simulated temperature and current density distributions are presented and discussed.

KEY WORDS: finite-element method; high temperature; millisecond pulse-heating; modeling; numerical simulation.

1. INTRODUCTION

In the late 1960s, millisecond pulse-heating experiments were developed by a research group led by A. Cezairliyan at the National Institute of Standards and Technology (NIST), Gaithersburg, Maryland, U.S.A. (at that

[1] Paper presented at the Seventh International Workshop on Subsecond Thermophysics, October 6-8, 2004, Orléans, France.

[2] Österreichisches Gießerei-Institut, Parkstraße 21, 8700 Leoben, Austria.
[3] To whom correspondence should be addressed. E-mail: kaschnitz.ogi@unileoben.ac.at
[4] Institut für Struktur- und Funktionskeramik, Montanuniversität Leoben, Peter-Tunner-Straße 5, 8700 Leoben, Austria.

time the National Bureau of Standards (NBS), Washington, DC, U.S.A.) to measure multiple thermophysical properties [1, 2]. The method leads to an unsurpassed accuracy for selected properties at very high temperatures and is even suitable to characterize reference materials. However, due to the self-heating by an electrical current, the method is restricted to electrically conducting materials, generally metals and alloys.

Several research groups have adapted the methodology to properties such as electrical resistivity, heat capacity, melting temperature, normal spectral and hemispherical total emissivity, thermal expansion, and others. A review on pulse calorimetry is given by Righini et al. [3]; more recent work is described by our research group [4] and by Dai et al. [5].

The original technique is based on rapid resistive heating of a tubular specimen by an electrical current and simultaneously measuring the pertinent quantities with at least millisecond resolution. The temperature development during heating and subsequent cooling is measured by a high-speed pyrometer. It is focused on a blackbody hole in the center part of the specimen. In order to achieve a uniform cross section along the entire specimen, a flat section is machined on the surface of the specimen next to the blackbody hole (Fig. 1).

However, the method assumes no significant temperature gradients along the cross section of the specimen (long thin-rod approximation), as diffusive heat transfer to the surface is not considered. This influence

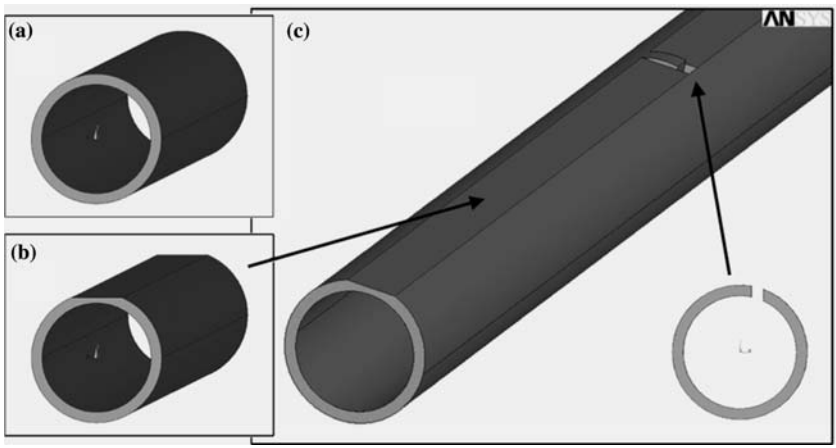

Fig. 1. Geometry of the three different models: (a) simple tubular specimen; (b) tubular specimen with flat; (c) tubular specimen with blackbody hole and flat (dimensions of Refs. 7 and 8: length, 80 mm; outer diameter, 6.35 mm; inner diameter, 5.33 mm; rectangular hole, $1.06 \times 0.56\,\text{mm}^2$).

of the surface radiation on temperature loss at the surface of a tungsten specimen including the diffusive heat transport from the inside towards the surface was simulated by Spišiak et al. [6] with a one-dimensional model of cylindrical cross section.

Also, the cross section of the specimen is not exactly uniform as a result of (a) the flat along almost the entire specimen and (b) the opening hole used as a blackbody source causing a distortion of the electrical current density in that region. This leads to a nonuniform temperature distribution especially in the region of the blackbody hole. In order to simulate this influence, a full three-dimensional finite-element analysis was made to investigate these limitations of the millisecond pulse-heating technique. A commercial program (ANSYS) has been used for a highly nonlinear finite-element analysis taking into account temperature-dependent material properties as well as heat transport by radiation. The geometry of the specimens refers to the work of Cezairliyan and McClure on tungsten [7] and Cezairliyan and Miiller on titanium [8]. Tungsten was selected because of the extended temperature range up to 3600 K (high temperature radiation losses) and titanium because of its relative low thermal conductivity (low diffusive heat transport).

2. MODEL

Three different geometries are considered in order to introduce stepwise the effect of different geometrical disturbances (Fig. 1):

(a) simple tubular specimen (outer diameter, 6.35 mm; inner diameter, 5.33 mm; length, 80 mm)

(b) tubular specimen with a flat (the cross section is reduced by 0.299 mm^2; the wall thickness has a minimum value of 0.31 mm)

(c) tubular specimen with a blackbody hole (width, 0.56 mm; height, 1.09 mm; rectangular shape) and with flats outside the blackbody region to maintain uniform cross section along the entire specimen.

For these geometries, the heat equation including the following physical phenomena are considered: (a) heat generation by the electrical current, (b) diffusive heat transport in the specimen, and (c) radiative heat transport at all (outer and inner) surfaces of the specimen. The heat equation is coupled with the Maxwell equation describing the electrical field and current density. The thermal expansion of the specimen, and the related change in geometry of approximately 2%, are not considered. The initial skin effect and the Seebeck effect are assumed to be negligible.

The geometry, as well as the boundary and initial conditions, were chosen to match as close as possible the experiments of Refs. 7 and 8. The temperature-dependent material properties of tungsten (heat capacity, electrical resistivity, thermal conductivity, and hemispherical total emissivity) are taken from different sources [7, 9, 10]; the corresponding properties of titanium originate from Refs. 8 and 10–14. The outer surfaces and those parts of the inner surfaces with a view to the outside are radiating against a surrounding temperature of 20°C. Since thermal expansion is not considered in the model, the temperature dependence of the density is not taken into account. The room temperature value of density used here is taken from Ref. 10. With a constant current of 2200 A for tungsten and a current of 800 A for titanium, a realistic heating time of slightly more than 500 ms from room temperature to a state close to melting was obtained. After the heating period, the current is switched off and the specimen cools due to the heat loss by radiation for another 200 ms.

3. MESH OF THE GEOMETRY

The geometry was meshed with linear brick elements with two degrees of freedom (temperature and voltage). The two models of (a) the simple tube and (b) the tube with a flat have approximately 20,000 elements; the model (c) with the blackbody hole and flats was refined in the region of the hole, leading to more than 100,000 elements.

Figure 2 shows the mesh of the geometry of the tubular specimen with the blackbody hole and flat. The diameter of the tube is divided in 60 sections and 12 layers. In the axial direction, the tube is divided in 30 sections. The mesh in the region of the blackbody hole is refined by a factor of 2–6. When meshing with brick elements, the curved surface of the tube is replaced by plane surfaces. In order to compensate for this meshing effect, the cross sections in the region of the flat and the blackbody hole were exactly matched by slightly changing the dimensions of the flat, keeping the cross section constant along the entire mesh.

4. NUMERICAL SIMULATION

The approximation of the descriptive system of equations was done by commercial finite-element software. Time-dependent results are temperature and voltage at each node of the mesh. The program ANSYS Multi-physics Version 8.0 running on a PC with an Intel Xeon processor (2.4 GHz) and 2 GB RAM and Windows XP as the operating system was used to calculate the solution. Due to the algorithm of the radiation solver, no symmetry of the geometry could be used. The simulations of the

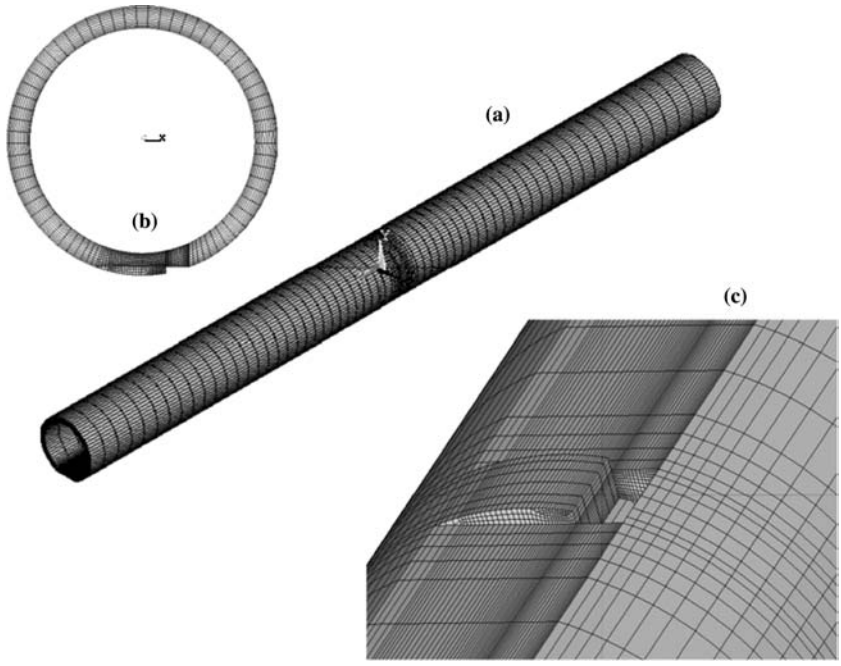

Fig. 2. Mesh of the tubular specimen with blackbody hole and flat: (a) entire model; (b) cross section of the model; (c) close-up to the blackbody hole.

simple tube and the tube with a flat took approximately 10 h; the simulation of the model with the blackbody hole and flats took more than 200 h.

Deviations of the simulation results from physical reality are due to different reasons: (a) simplifications of physical phenomena (e. g., thermal expansion, Lorentz force); (b) simplifications of initial and boundary conditions (e. g., constant electrical current, material properties); (c) simplifications of the geometry by meshing (approximation of curved surfaces by flat surfaces); and (d) approximation by a numerical solution (residuals and rounding). In order to check the principal validity of the model, our three-dimensional model has been calculated with the same dimensions and very similar boundary conditions as the one-dimensional model of Spišiak et al. [6], leading to very similar results.

5. RESULTS

The temperature distribution of the simple tungsten tube at a heating time of 560 ms (close to melting) is shown in Fig. 3. There is a temperature difference of approximately 5°C between the inner and outer surfaces of

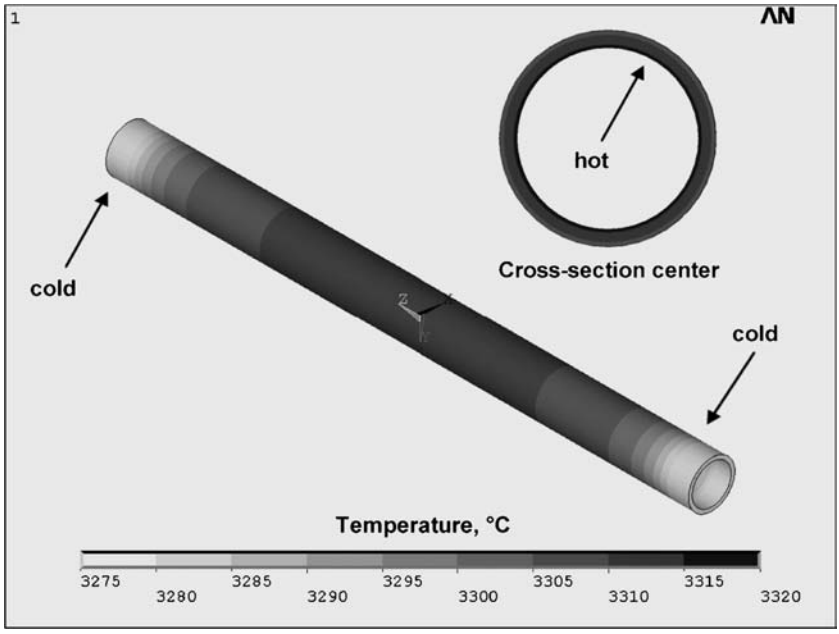

Fig. 3. Temperature distribution of a simple-tube tungsten specimen at a heating time of approximately 500 ms at high temperature close to melting.

the tube. A gradient of approximately 50°C develops along the axial direction, but this is outside the measurement region, which is defined in a real experiment by the voltage probes. Figure 4 shows the temperature distribution in the tungsten tube with a flat at a similar time, the gradient along the cross section increases to 10°C due to the different wall thickness along the diameter.

The temperature distribution becomes increasingly more inhomogeneous with the additional blackbody hole. Figure 5 shows the temperature distribution in the vicinity of the blackbody hole at a heating time of 540 ms. A temperature gradient on the order of 130°C has developed with a hot spot at one side of the hole and a cold spot at the opposite side.

The current density (derived from the voltage distribution, taking into account the temperature dependence of the resistivity) in the vicinity of the blackbody hole at the heating time of 540 ms is shown in Fig. 6. Steep gradients of the current density can be seen; the absolute values differ by a factor of approximately 7. These gradients in current density cause the non-uniform temperature distribution.

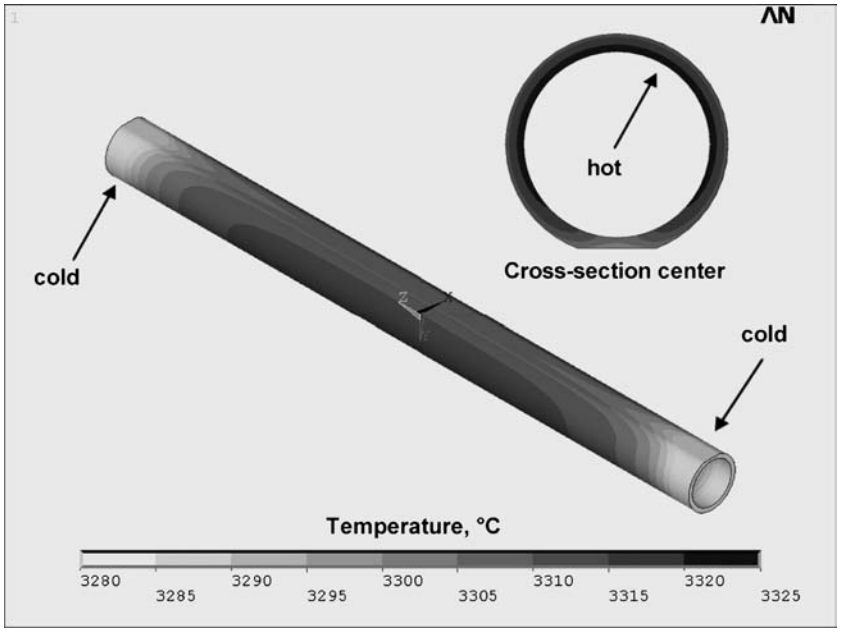

Fig. 4. Temperature distribution of a flattened-tube tungsten specimen at a heating time of approximately 500 ms at high temperature close to melting.

In order to test the influence of the temperature gradients on the obtained results of a real millisecond pulse-heating experiment, the measurement procedure was also simulated. The voltage difference between two defined nodes along a portion of the specimen and the temperature at a node at the opposite side of the blackbody hole were time-resolved (Fig. 7). With this data, the specific heat capacity and electrical resistivity read were calculated using the equations for power balance and Ohm's law [4, 14]. Comparisons of the resulting specific heat capacity and electrical resistivity with the simulation input show a small difference of 0.1% in electrical resistivity and a deviation of 1% in specific heat capacity (Fig. 8). The temperature measurement spot at the opposite side of the blackbody hole is somewhat arbitrary, but it is a necessary assumption as the simulation (at the present stage) cannot calculate the averaged temperature as seen by a pyrometer.

In a real experiment, the temperature, measured by a radiation pyrometer, is determined by a local surface temperature and the effective emissivity. Thermal radiation measured by a pyrometer will consist of the self-radiation of the surface (defined by the temperature and spectral

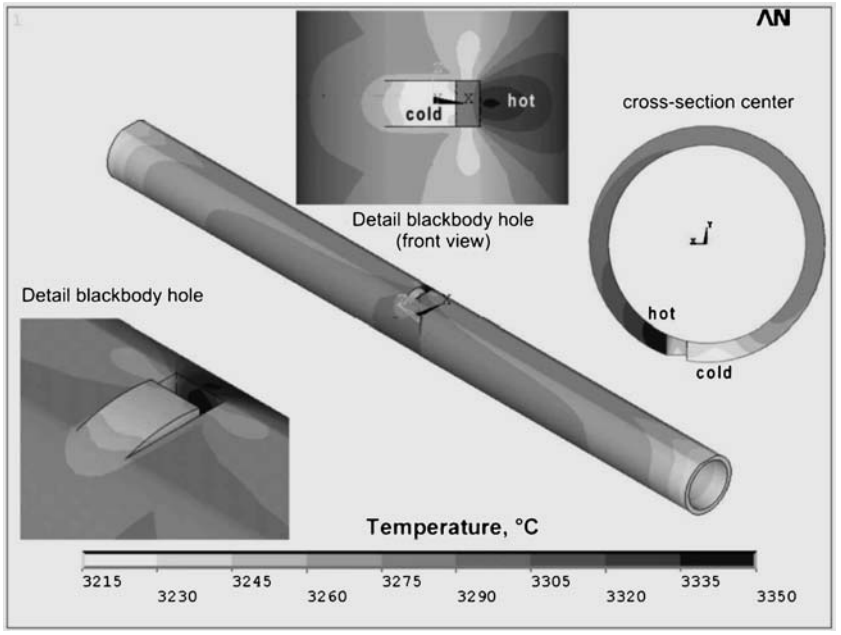

Fig. 5. Temperature distribution of a tube-shaped tungsten specimen with blackbody hole and flats at a heating time of approximately 500 ms at high temperature close to melting.

emissivity of the metal—the latter is, usually, in the range of 0.3–0.4 depending on the wavelength and the metal) and the reflected light emitted by the inner surface of the tube. Thus, the effective emissivity is, actually, the reflected light emitted by the inner surface of the tube. As the effective emissivity is close to one, it is obvious that 2/3 of the radiation entering the pyrometer optics is the reflected light emitted by the surface of the wall, having a higher mean temperature than the measuring point. Due to this effect, the actually measured temperature is higher and, therefore, one can presume that the deviations between real measurements and simulated measurements are much smaller.

All the deviations in temperature and current density are very similar but smaller for the titanium specimens. In general, the effect of the disturbance of the uniformity of the cross section in the vicinity of the blackbody hole contributes more to the distortion of the temperature field than the effect of the radiation loss at the surface and the lack of heat transport by a finite thermal conductivity.

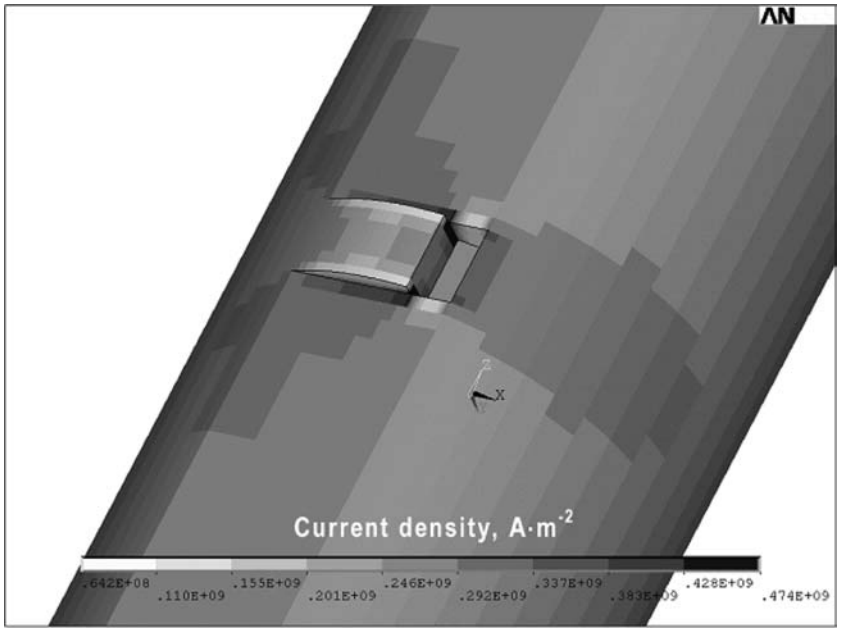

Fig. 6. Current density distribution of a tube-shaped tungsten specimen with blackbody hole and flats at a heating time of approximately 500 ms at high temperature close to melting (detail in the vicinity of the blackbody hole).

6. DISCUSSION AND OUTLOOK

The performed three-dimensional finite-element analysis of a millisecond pulse-heating experiment shows significant deviations from the assumption of a uniform temperature field along and across the specimen. The distortion of the current density field can cause temperature differences in the range of 100°C and steep temperature gradients. A high quality pyrometer with a very small viewing spot and a limited size-of-source effect is necessary to avoid radiation pick-up from the hottest and coldest spots close to the blackbody hole. However, due to the relative small region of major disturbances in the current distribution and the temperature field, the influence on the obtained results in the (simulated) measurement is limited.

Well balanced geometrical dimensions (inner and outer diameter, size of blackbody hole, and flat) seem to be crucial to obtain a relative uniform temperature distribution. If the wall thickness of the specimen is too large, the necessary heat transport to the radiating surface is too low, and a temperature gradient between the inner and outer surfaces develops. However,

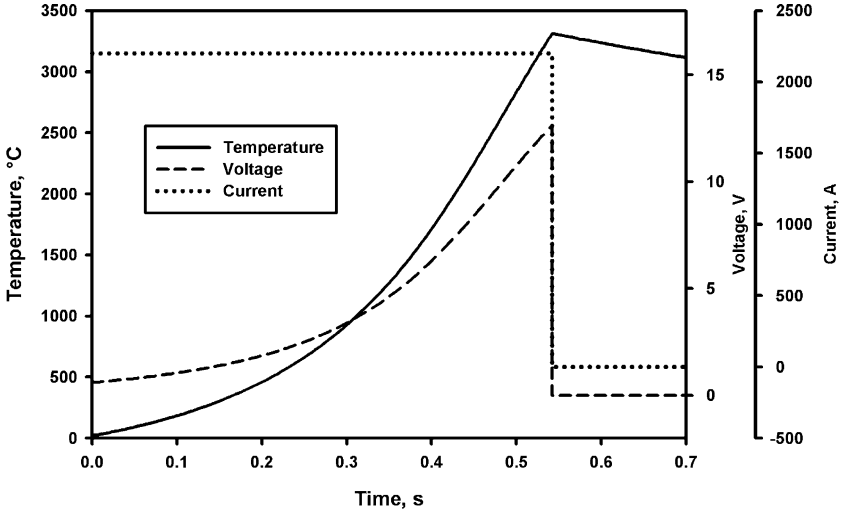

Fig. 7. Simulated temperature of a node at the opposite side of the blackbody hole of the tungsten specimen, voltage drop along a defined portion of the specimen, and current through the specimen as a function of time at heating and cooling.

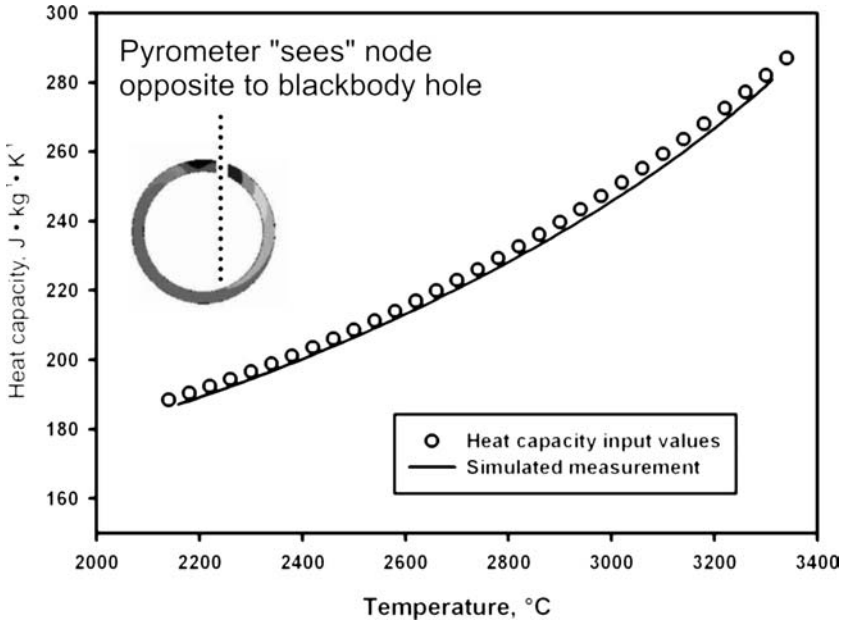

Fig. 8. Simulation input values of specific heat capacity and electrical resistivity as a function of temperature compared with results of a simulated measurement.

if the wall thickness is lowered too far, the influence of the flat increases and the temperature gradient increases around the circular cross section.

In order to continue this work, temperature measurements with a thermo-camera (to obtain time and spatial resolution) on pulse-heated specimens are planned and subsequently compared to the results of simulations. Another important question is the actual view of the pyrometer pointing at the blackbody hole. Future simulations could take into account the temperature radiation pick-up of different regions of the specimen by the pyrometer.

ACKNOWLEDGMENT

This work was supported by the Forschungsförderungsfonds für die gewerbliche Wirtschaft (FFF), Vienna, Austria under contract No. 807706.

REFERENCES

1. A. Cezairliyan, *J. Res. Natl. Bur. Stand. (U.S.)* **75C**: 7 (1971).
2. A. Cezairliyan, M. S. Morse, H. A. Berman, and C. W. Beckett, *J. Res. Natl. Bur. Stand. (U.S.)* **74A**: 65 (1970).
3. F. Righini, G. C. Bussolino, and J. Spišiak, *Thermochim. Acta* **347**: 93 (2000).
4. P. Reiter and E. Kaschnitz, *High Temp. High Press*. **33**: 505 (2001).
5. J. M. Dai, Y. Fan, and Z. X. Chu, *Int. J. Thermophys*. **23**: 1401 (2002).
6. J. Spišiak, F. Righini, and G. C. Bussolino, *Int. J. Thermophys*. **22**: 1241 (2001).
7. A. Cezairliyan and J. L. McClure, *J. Res. Natl. Bur. Stand. (U.S.)* **75A**: 283 (1971).
8. A. Cezairliyan and A. P. Miiller, *High Temp. High Press*. **9**:319 (1977).
9. G. K. White and M. L. Minges, *Int. J. Thermophys.* **18**:1269 (1997).
10. W. Blanke, *Thermophysikalische Stoffgrößen* (Springer-Verlag, Berlin, 1989).
11. P. D. Desai, *Int. J. Thermophys.* **8**:781 (1987).
12. Y. S. Touloukian, R. W. Powell, C. Y. Ho, and P. G. Klemens, eds., *Thermophysical Properties of Matter*, Vol. 1, *Thermal Conductivity – Metallic Elements and Alloys* (Plenum, New York, 1970).
13. K. D. Maglić and D. Z. Pavičić, *Int. J. Thermophys.* **22**: 1833 (2001).
14. E. Kaschnitz and P. Reiter, *J. Therm. Anal. Calorim*. **64**: 351 (2001).